confirm the effectiveness of the proposed approach, which may be successfully employed early in the design process.

References

[1]Ashkenas, I. L., and McRuer, D. T., "Optimization of Flight-Control, Airframe System," *Journal of Aerospace Science*, Vol. 27, No. 3, 1960, pp. 197–218.

[2]Lutze, F. H., Durham, W. C., and Mason, W. H., "Unified Development of Lateral–Directional Departure Criteria," *Journal of Guidance, Control, and Dynamics*, Vol. 19, No. 2, 1996, pp. 489–493.

[3]McRuer, D. T., Ashkenas, I. L., and Graham, D., *Aircraft Dynamics and Automatic Control*, Princeton Univ. Press, Princeton, NJ, 1973, pp. 354, 367–378, 402.

[4]Heffley, R. K., and Jewell, W. F., "Aircraft Handling Qualities Data," Technical Rept. NASA CR-2144, Systems Technology, Inc., Dec. 1972.

[5]Livneh, R., "Improved Literal Approximation for Lateral–Directional Dynamics of Rigid Aircraft," *Journal of Guidance, Control, and Dynamics*, Vol. 18, No. 4, 1995, pp. 925–927.

[6]Duncan, W. J., *The Principles of the Control and Stability of Aircraft*, Cambridge Univ. Press, London, 1952, pp. 117–125.

[7]Weissman, R., "Preliminary Criteria for Predicting Departure Characteristics/Spin Susceptibility of Fighter-Type Aircraft," *Journal of Aircraft*, Vol. 10, No. 4, 1973, pp. 214–219.

[8]Ananthkrishnan, N., Shah, P., and Unnikrishnan, S., "Approximate Analytical Criterion for Aircraft Wing Rock Onset," *Journal of Guidance, Control, and Dynamics*, Vol. 27, No. 2, 2004, pp. 304–307.

[9]Franklin, G. F., Powell, J. D., and Emami-Naeini, A., *Feedback Control of Dynamic Systems*, 4th ed., Prentice–Hall, Upper Saddle River, NJ, 2002, p. 166.

[10]Fan, Y., Lutze, F. H., and Cliff, E. M., "Time-Optimal Lateral Maneuvers of an Aircraft," *Journal of Guidance, Control, and Dynamics*, Vol. 18, No. 5, 1995, pp. 1106–1112.

Limit Cycles and Domain of Stability in Unsteady Aeroelastic System

Sushma Gujjula,* Sahjendra N. Singh,† and Woosoon Yim‡
University of Nevada, Las Vegas, Nevada 89154-4026

Introduction

AEROELASTIC systems exhibit a variety of phenomena including instability, limit-cycle oscillation (LCO), and even chaotic vibration.[1] An excellent survey paper by Mukhopadhyay[2] provides a historical perspective on analysis and control of aeroelastic systems. Studies related to prediction of flutter instability theory have been done.[1,3–8] In this Note, the existence of LCO and the domain of stability (attraction) in prototypical aeroelastic wing sections are examined. Unlike Ref. 8, the aeroelastic model considered here includes the unsteady aerodynamics based on Theodorsen's theory.[9] The model includes a structural nonlinearity of fifth degree in the pitch degree of freedom. The chosen dynamic model describes the nonlinear plunge and pitch motion of a wing.[4,5] The dual-input describing functions (DIDFs)[10] of the nonlinearity for asymmetric oscillations are used for the prediction of unstable and stable limit cycles. For the case when the origin is stable, the quadratic Lyapunov method (see Ref. 11) is used to compute the domain of attraction. Analytical expressions for the computation of biases, amplitudes, and frequencies of oscillation of the pitch and plunge responses are obtained. The orbital stability of the LCO using the Nyquist criterion is established, and it is shown that both unstable as well as stable limit cycles exist when the origin is exponentially stable.

Aeroelastic Model

The prototypical aeroelastic wing section is shown in Fig. 1. The governing equations of motion of the aeroelastic system are given by[4,5]

$$\begin{bmatrix} m_t & m_w x_\alpha b \\ m_w x_\alpha b & I_\alpha \end{bmatrix}\begin{bmatrix} \ddot{h} \\ \ddot{\alpha} \end{bmatrix} + \begin{bmatrix} c_h & 0 \\ 0 & c_\alpha \end{bmatrix}\begin{bmatrix} \dot{h} \\ \dot{\alpha} \end{bmatrix} + \begin{bmatrix} k_h & 0 \\ 0 & k_\alpha(\alpha) \end{bmatrix}\begin{bmatrix} h \\ \alpha \end{bmatrix} = \begin{bmatrix} -L(t) \\ M(t) \end{bmatrix} \tag{1}$$

where α is the pitch angle, b is the semichord of the wing, h is the plunge displacement, m_w and m_t are the mass of the wing and the total mass, I_α is the moment of inertia, and x_α is the nondimensionalized distance of the center of mass from the elastic axis. The lift $L(t)$ and moment $M(t)$ represent the unsteady aerodynamics, which are functions of position, velocity, acceleration, and time prehistory of the vortex wave. The lift and moment are acting at the elastic axis of the wing. Here c_α and c_h are the pitch and plunge damping coefficients, k_{h0} is the plunge spring constant, and $k_\alpha(\alpha)$ is the nonlinear function associated with the pitch spring. For purposes of illustration, the function $\alpha k_\alpha(\alpha)$ is considered as a polynomial nonlinearity of fifth degree. This is given by $\alpha k_\alpha(\alpha) = \alpha(k_{\alpha_0} + k_{\alpha_1}\alpha + k_{\alpha_2}\alpha^2 + k_{\alpha_3}\alpha^3 + k_{\alpha_4}\alpha^4)$.

Theodorsen[9] derived the expressions for lift and moment, assuming harmonic motion of the airfoil, of the form[5]

$$\begin{aligned} -L(t) &= -\rho b^2 s_p(U\pi\dot{\alpha} + \pi\ddot{h} - \pi ba\ddot{\alpha}) \\ &\quad - 2\pi\rho U b s_p C(k)\left[U\alpha + \dot{h} + b\left(\tfrac{1}{2} - a\right)\dot{\alpha}\right] \\ M(t) &= -\rho b^2 s_p\left\{\pi\left(\tfrac{1}{2} - a\right)Ub\dot{\alpha} + \pi b^2\left(\tfrac{1}{8} + a^2\right)\ddot{\alpha} - a\pi b\ddot{h}\right\} \\ &\quad + 2\rho U b^2 \pi s_p\left(\tfrac{1}{2} + a\right)C(k)\left[U\alpha + \dot{h} + b\left(\tfrac{1}{2} - a\right)\dot{\alpha}\right] \end{aligned} \tag{2}$$

where s_p is the span and a is nondimensionalized distance from the midchord to the elastic axis and U is freestream velocity. Jones

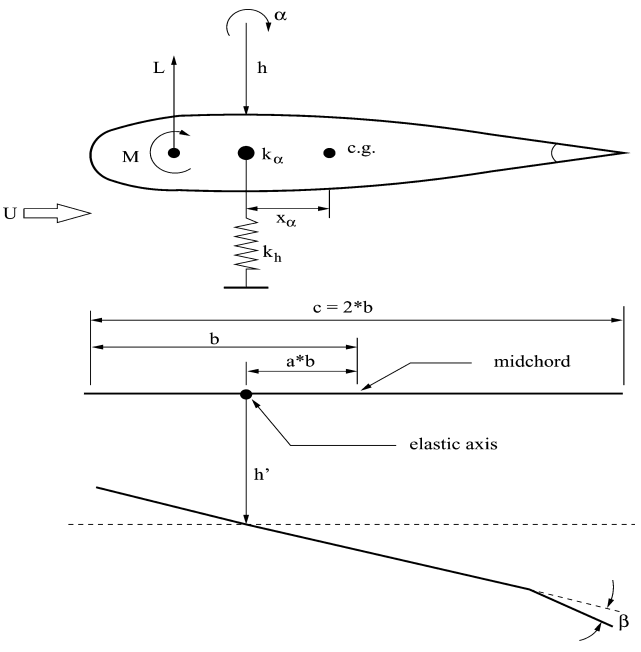

Fig. 1 Aeroelastic model.

Received 18 December 2003; revision received 19 February 2004; accepted for publication 20 February 2004.

*Graduate Student, Electrical and Computer Engineering.
†Professor, Electrical and Computer Engineering.
‡Professor, Mechanical Engineering.

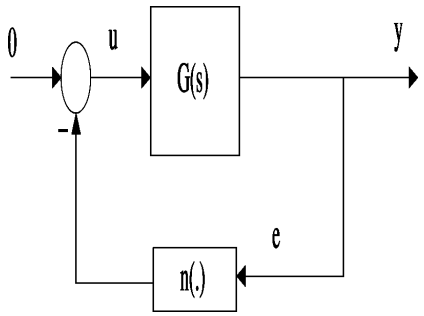

Fig. 2 Feedback system.

developed an approximation to Theodorsen's function $C(k)$ for simplicity in computation, which can be written as (see Ref. 5)

$$C(s) = 0.5 + \frac{a_1 s + a_0}{s^2 + b_1 s + b_0} \tag{3}$$

where s is the Laplace variable and $a_1 = 0.1080075(U/b)$, $a_0 = 0.006825U^2 b^{-2}$, $b_1 = 0.3455(U/b)$, and $b_0 = 0.01365U^2 b^{-2}$.

It will be convenient to obtain a state variable form of the complete model. Theodorsen's function $C(s)$ can be treated as a second-order transfer function of a filter and can be realized as

$$\dot{x}_{f1} = x_{f2}$$

$$\dot{x}_{f2} = -b_0 x_{f1} - b_1 x_{f2}[U\alpha + \dot{h} + b(0.5 - a)\dot{\alpha}] \tag{4}$$

Define the state vector including the filter states as $\boldsymbol{x} = (h, \alpha, \dot{h}, \dot{\alpha}, x_{f1}, x_{f2})^T \in R^6$. The complete system including Eqs. (1) and (4) has a state variable representation of the form

$$\dot{=} A\boldsymbol{x} - Bk_{n_\alpha}(\alpha) \tag{5}$$

where A and B are appropriate matrices and

$$k_{n\alpha}(\alpha) = \alpha\left(k_{\alpha_1}\alpha + k_{\alpha_2}\alpha^2 + k_{\alpha_3}\alpha^3 + k_{\alpha_4}\alpha^4\right) \tag{6}$$

Define $u = -n(e)$, with $e = y = \alpha = C_a\boldsymbol{x}$, where one has $n(e) = e(k_{\alpha_1}e + k_{\alpha_2}e^2 + k_{\alpha_3}e^3 + k_{\alpha_4}e^4)$ and $C_a = [0, 1, 0, 0, 0, 0]$. Then the system (5) can be represented as a negative feedback system as shown in Fig. 2. The transfer function $G(s)$ relating the output y and u can be written as

$$\hat{y}(s)/\hat{u}(s) = C_a(sI_{6\times 6} - A)^{-1}B = G(s) = n_1(s)/d_1(s) \tag{7}$$

where $\hat{}$ denotes the Laplace transform of signals.

Describing Function and LCO

In this section, the describing function method is used for the prediction of limit cycles. For the limit-cycle analysis, first the quasi-linear approximation of the nonlinear operator by harmonic balancing must be obtained. For the aeroelastic model, numerical results show that the steady-state oscillations are periodic, but a nonzero average exists.

In the aeroelastic system, let us assume that there exists an LCO and that the pitch angle $y = \alpha$ and the plunge displacement are sinusoidal functions that have nonzero average. Let the input signal, $e = y = \alpha$, to the nonlinear block and the plunge displacement in the steady-state be of the form

$$e(t) = B_\alpha + A_\alpha \sin(\omega t), \qquad h(t) = B_h + A_h \sin(\omega t + \theta) \tag{8}$$

where B_k, A_k, and ω are the bias, amplitude, and frequency of LCO, respectively, $k \in \{\alpha, h\}$. Here θ is the phase shift in the plunge response with respect to the pitch response.

Because e is the sum of the two signals (a constant and a sinusoidal function), one needs to obtain the DIDF. The output $n(e)$ of the nonlinear operator is a periodic signal and is given by

$$n(e) = \sum_{j=1}^{4} k_{\alpha_j}[B_\alpha + A_\alpha \sin(\omega t)]^{j+1} \tag{9}$$

The periodic signal $n(e)$ has its fundamental frequency ω and can be represented as a Fourier series that contains higher harmonics. In the following approximate analysis, for simplicity a quasi-linear approximation of the nonlinear element is obtained by retaining only the fundamental and constant terms of its output and higher harmonics are ignored. Thus, the output of the nonlinear block is approximated as

$$n_a(e) = N_0(B_\alpha, A_\alpha) + A_\alpha N(B_\alpha, A_\alpha)\sin(\omega t) \tag{10}$$

The Fourier coefficients N_0 and N, which are nonlinear functions of the bias and amplitude, have been derived in Ref. 8. (These are given in the Appendix.) The DIDFs associated with the constant and the sinusoidal inputs are $N_0 B_\alpha^{-1}$ and N, respectively. The steady-state output of the linear block due to the approximate input $u = -n_a$ is

$$y(t) = -G(j0)N_0(B_\alpha, A_\alpha) - |G(j\omega)|A_\alpha N(B_\alpha, A_\alpha)\sin[\omega t + \angle G(j\omega)] = -G(j0)N_0(B_\alpha, A_\alpha) - A_\alpha N(B_\alpha, A_\alpha) \times [G_r(\omega)\sin(\omega t) + G_i(\omega)\cos(\omega t)] \tag{11}$$

where $G(j\omega) = G_r(\omega) + jG_i(\omega)$, that is, G_r is the real part and G_i is the imaginary part of the transfer function G.

Because the output of the linear block is the input to the nonlinear block ($e = y$), it follows from Eqs. (8) and (11) that

$$G(j0)N_0(B_\alpha, A_\alpha) = -B_\alpha \tag{12}$$

$$N(B_\alpha, A_\alpha)G_r(\omega) = -1 \tag{13}$$

$$N(B_\alpha, A_\alpha)G_i(\omega) = 0 \tag{14}$$

If the LCO exists, then Eqs. (12–14) are necessarily satisfied. Solving these equations gives the bias term and the amplitude and frequency of oscillation. An equivalent representation of Eqs. (13) and (14) takes a form of complex equation given by

$$1 + N(B_\alpha, A_\alpha)[G_r(j\omega) + jG_i(j\omega)] = 1 + N(B_\alpha, A_\alpha)G(j\omega) = 0 \tag{15}$$

Equation (15) has a geometric interpretation. Indeed, the values of B_α and A_α corresponding to the point of intersection of the Nyquist diagram of $G(s)$ and the plot of $[-1/N^{-1}(B_\alpha, A_\alpha)]$ are the solutions of Eqs. (13) and (14).

Now that B_α, A_α, and ω have been obtained, one can proceed to solve the oscillation parameters for the plunge degree of freedom. Defining the output matrix $C_p = [1, 0_{1\times 5}]$, one has $h = C_p\boldsymbol{x}$, and the transfer function relating h to u is

$$G_p(s) = C_p(sI_{6\times 6} - A)^{-1}B = \hat{h}(s)/\hat{u}(s) \tag{16}$$

For computing the bias and fundamental component of the periodic function h, it is necessary to substitute

$$u = -n_a(e) = -N_0(B_\alpha, A_\alpha) - A_\alpha N(B_\alpha, A_\alpha)\sin(\omega t) \tag{17}$$

in Eq. (16). Then it easily follows that, in the steady state, the plunge displacement is given by

$$h(t) = -G_p(0)N_0(B_\alpha, A_\alpha) - A_\alpha N(B_\alpha, A_\alpha)|G_p(j\omega)|\sin[\omega t + \angle G_p(j\omega)] \tag{18}$$

In view if Eqs. (8) and (18), comparing similar terms gives

$$B_h = -G_p(0)N_0(B_\alpha, A_\alpha)$$

$$A_h\cos(\theta) = -A_\alpha N(B_\alpha, A_\alpha)G_{pr}(j\omega)$$

$$A_h\sin(\theta) = -A_\alpha N(B_\alpha, A_\alpha)G_{pi}(j\omega) \tag{19}$$

where $G_p(j\omega) = G_{pr}(j\omega) + jG_{pi}(j\omega)$. Equation (19) is solved to obtain A_h and θ.

Domain of Stability

Interestingly, there exists flutter even though the equilibrium point $\boldsymbol{x} = 0$ is exponentially stable.[7] In such cases, it is of interest to determine the domain of stability surrounding the origin. Suppose that for a given flow velocity, the matrix A is Hurwitz. Then for any given positive definite symmetric matrix Q (denoted as $Q > 0$), there exists a unique solution of the Lyapunov equation (see Ref. 11)

$$A^T P + PA = -Q \tag{20}$$

and the matrix $P > 0$. For analyzing stability of the nonlinear system Eq. (5), consider a quadratic Lyapunov function

$$V(\boldsymbol{x}) = \boldsymbol{x}^T P\boldsymbol{x} \tag{21}$$

Taking the derivative of $V(\boldsymbol{x})$ along the solution of Eq. (5) gives

$$\dot{V}(\boldsymbol{x}) = \boldsymbol{x}^T[A^T P + PA]\boldsymbol{x} - 2\boldsymbol{x}^T PBk_{n\alpha}(\alpha)$$

$$\leq -\boldsymbol{x}^T Q\boldsymbol{x} + 2\|\boldsymbol{x}\|\|PB\||k_{n\alpha}(\alpha)| \tag{22}$$

where $\|\cdot\|$ denotes the Euclidean norm. The nonlinear function can be bounded as

$$|k_{n\alpha}(\alpha)| = |\alpha|\left|\left(k_{\alpha_1}\alpha + k_{\alpha_2}\alpha^2 + k_{\alpha_3}\alpha^3 + k_{\alpha_4}\alpha^4\right)\right| \leq \|\boldsymbol{x}\|\mu(\alpha) \tag{23}$$

where $\mu(\alpha) \doteq |(k_{\alpha_1}\alpha + k_{\alpha_2}\alpha^2 + k_{\alpha_3}\alpha^3 + k_{\alpha_4}\alpha^4)|$.

For any $n \times n$ matrix $M > 0$, one has $\lambda_{\min}(M)\|\boldsymbol{x}\|^2 \leq \boldsymbol{x}^T M\boldsymbol{x} \leq \lambda_{\max}(M)\|\boldsymbol{x}\|^2$, where $\lambda_{\min}$ (max) denotes minimum (maximum) eigenvalue of M. Using Eq. (23) in Eq. (22) gives

$$\dot{V}(\boldsymbol{x}) \leq -\|\boldsymbol{x}\|^2[\lambda_{\min}(Q) - 2\|PB\|\mu(\alpha)] \tag{24}$$

For the nonlinear function $\mu(\alpha)$, one can find an interval $[-\alpha^*, \alpha^*] \in R$ centered at zero such that

$$\mu(\alpha) \leq \lambda_{\min}(Q)/(2\|PB\|) \doteq r^* \tag{25}$$

For $\alpha \in [-\alpha^*, \alpha^*]$, consider an ellipsoid E defined as $E(\gamma) = \{x \in R^6 : x^T Px = \gamma\}$, where $\gamma > 0$. Define a region surrounding the origin as $\Omega = \{x \in R^6 : |\alpha| \leq \alpha^*\}$.

We are interested in obtaining the largest ellipsoid contained in Ω. This can be obtained by minimizing $\boldsymbol{x}^T P\boldsymbol{x}$ subject to the constraint $\alpha = |\alpha^*|$. The optimal solution is obtained by minimizing

$$J = \boldsymbol{x}^T Px - \lambda\left(x_2 - \alpha^*\right) \tag{26}$$

where λ is the Lagrange multiplier. The necessary conditions for optimality are

$$\frac{\mathrm{d}J}{\mathrm{d}\boldsymbol{x}} = 2P\boldsymbol{x} - \lambda e_2 = 0, \qquad \frac{\mathrm{d}J}{\mathrm{d}\lambda} = x_2 - \alpha^* = 0 \tag{27}$$

where $e_2 = (0, 1, 0_{1\times 4})^T$. Solving Eq. (27) gives the optimal solution

$$\boldsymbol{x}^* = \lambda P^{-1}e_2/2 \tag{28}$$

Because $x_2^* = \alpha^*$, according to Eq. (28), one has

$$\lambda = 2\alpha^*/p_{i22} \tag{29}$$

where p_{i22} is the element in the second row and second column of P^{-1}. The optimal value of V is then

$$V = (P\boldsymbol{x}^*)^T P\boldsymbol{x}^* = \lambda^2 e_2^T P^{-1}PP^{-1}e_2/4 = \alpha^{*2}/p_{i22} \doteq \gamma^* \tag{30}$$

Then it follows that $\dot{V}(\boldsymbol{x}) < 0$, for all $\boldsymbol{x} \in E(\gamma) - \{0\}$, where $\gamma < \gamma^*$. Because $V(\boldsymbol{x})$ is a positive definite function, invoking the Lyapunov theorem (see Ref. 11), one concludes that any trajectory that begins from $\boldsymbol{x}(0) \in E(\gamma)$, $\gamma < \gamma^*$, converges exponentially to the origin and flutter cannot exist. The region interior of the ellipsoid $E(\gamma^*)$ is an estimate of the domain of stability. The computation of a region of stability using the result of this section is presented in the next section.

This section presents numerical results. The model parameters are given in the Appendix.

Amplitudes and Biases of Limit Cycles: Stable and Unstable Origin

The DIDF method is used for the prediction of limit cycles for various values of U and a. The ampitudes, biases, and frequencies of oscillation of limit cycles are obtained by solving Eqs. (12–14) for a set of values of $a \in \{-0.4, -0.6, -0.8\}$ for each value of $U \in [12, 20]$ m/s and are plotted in Fig. 3. The actual values of the oscillation parameters are also obtained by numerical simulation of the open-loop system. Table 1 gives the predicted and actual values of the amplitudes and biases of the limit cycles for $U \in [15, 20]$ m/s and $a = -0.4$. It is seen that the amplitudes of oscillations, as well as magnitudes of biases, increase monotonically with velocity, but the bias angle is negative and the plunge bias is positive. It is seen that the predicted and acutal values are close. Of course, better approximations can be obtained by including higher harmonics of signals in the analysis but at the cost of increasing complexity.

Note that the origin is stable for $a = -0.4$, but it becomes unstable for $a = -0.8$. It is seen that the magnitudes of the plunge amplitude and bias, as well as the pitch bias, decrease as a gets closer to -1. It is seen that, for larger velocities, the pitch amplitude is smaller for $a = -0.8$ compared to $a = -0.4$ and -0.6. The amplitudes and frequencies of oscillations monotonically increase with velocity for each value of a.

Nyquist Diagram: Limit Cycles and Stability

Nyquist diagrams can be used to determine limit cycles and establish their stability.

Table 1 Predicted and actual (simulated) values of amplitude and bias for pitch and plunge oscillations for $a = -0.4$.

	U, m/s					
Parameter	15	16	17	18	19	20
Predicted A_α, deg	7.02505	7.36505	7.69165	8.0114	8.3283	8.645
Actual A_α, deg	6.9489	7.2790	7.5964	7.9065	8.2135	8.5203
Predicted A_h, m	0.01415	0.016045	0.018	0.02005	0.0222	0.02445
Actual A_h, m	0.0143	0.0162	0.0182	0.0202	0.0224	0.0247
Predicted B_α, deg	−0.16435	−0.17425	−0.18405	−0.1938	−0.2038	−0.2141
Actual B_α, deg	−0.1977	−0.2089	−0.2202	−0.2317	−0.2434	−0.2555
Predicted $B_h \times 10^{-3}$, m	0.15	0.155	0.2	0.25	0.30	0.3
Actual $B_h \times 10^{-3}$, m	0.1341	0.1617	0.1923	0.2263	0.2649	0.3082

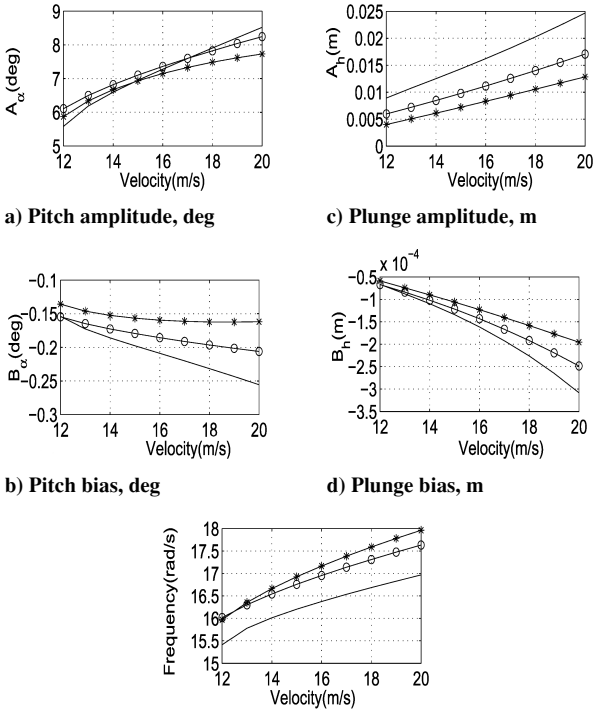

Fig. 3 Limit cycles, $U = [12, 20]$ m/s, and ——, $a = -0.4$; ○, $a = -0.6$; and ∗, $a = -0.8$.

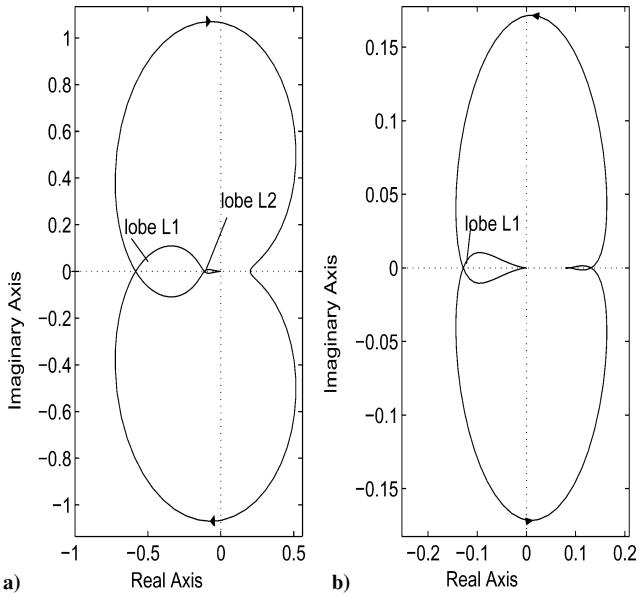

Fig. 4 Nyquist plots: a) origin stable, $U = 19.0625$ m/s, and $a = -0.4$ and b) origin unstable, $U = 19.0625$ m/s, and $a = -0.8$.

Numerical Results

Stable and Unstable Limit Cycles: Origin Stable

First we examine the orbital stability for $U = 19.0625$ m/s and $a = -0.4$, for which the origin is stable. For this case, A is Hurwitz. It turns out that in this case, for stability, according to the Nyquist criterion (see Ref. 11) $(-1/N)$ point must not be encircled by the Nyquist diagram because the open-loop system is stable. Figure 4 shows the Nyquist plot. Notice that for $a = -0.4$ the Nyquist diagram has two lobes (L1 and L2) centered along the negative real axis and intersects the $(-1/N)$ plot twice, first at a lower frequency ($\omega_l = 13.8099$ rad/s) and then at a higher frequency ($\omega_h = 16.8369$ rad/s). Therefore, there exist two limit cycles. Solving Eqs. (12) and (13) gives the amplitudes and biases of the limit cycle, which are 3.4225 and -0.0979 deg for lower frequency and 8.2327 and -0.2441 deg for the higher frequency. It turns out that a stable limit cycle is not possible at the lower frequency (corresponding to the intersection point with the left lobe) because, as the value of A_α increases from the equilibrium value A^*_α, the $(-1/N)$ point enters the left lobe and is encircled twice in clockwise direction, which implies that the system becomes unstable. Thus, the amplitude of oscillation keeps on increasing until it reaches the value corresponding to the point of intersection of Nyquist diagram at the higher frequency with the right lobe. This intersection point gives a stable limit cycle, which can be explained as follows: Notice that in this case if A_α exceeds A^*_α the corresponding critical point $(-1/N)$ lies within the right lobe (L2). Figure 4a shows that the point $(-1/N)$ is encircled once in the clockwise and then in the counterclockwise direction, giving a net encirclement zero. Therefore, according to the Nyquist criterion, the system is stable and the amplitude starts decreasing until it reaches A^*_α. Of course, if $A_\alpha < A^*_\alpha$, the point $(-1/N)$ lies in the first lobe (L1), where it is unstable as required, and, therefore, A_α converges to A^*_α.

To verify the existence of the predicted limit cycles, simulation results for $U = 19.0625$ and $a = -0.4$ with the initial condition $\boldsymbol{x}(0) = (0, 4.07453 \text{ deg}, 0, 0, 0, 0)^T$ are obtained and plotted in Fig. 5. Figure 5 shows both the unstable LCO of smaller amplitude and the stable LCO of larger amplitude.

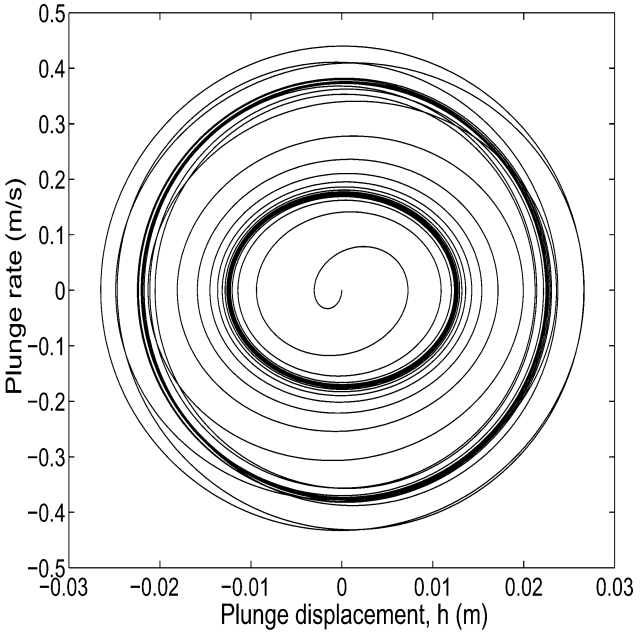

Fig. 5 Phase plane plot, h(meters)-$\dot{h}$(meters per second), $U = 19.0625$ m/s, and $a = -0.4$.

Stable Limit Cycle: Origin Unstable

Now we consider the case of unstable origin. The Nyquist diagram of $G(s)$ for $U = 19.0625$ m/s and $a = -0.8$ is shown in Fig. 4b. For the chosen value of U and a, the matrix A has two unstable eigenvalues. It is seen from Fig. 4b that the $(-1/N)$ point is enclosed twice in the counterclockwise direction by the Nyquist contour if $A_\alpha > A^*_\alpha$. Therefore, according to the Nyquist criterion, the limit cycles is orbitally asymptotically stable.

Domain of Stability: $U = 19.0625$ Meters per Second and $a = -0.4$

As shown in this case, limit cycles exist even though the origin is exponentially stable. However, because the system is exponentially stable (where A is Hurwitz), there exists a finite domain of stability surrounding the origin. Indeed for the choice of $\boldsymbol{x}(0) = [0, 3 \text{ deg}, 0, 0, 0, 0]^T$, $U = 19.0625$ m/s, and $a = -0.4$, the trajectory (not shown here) converges to the origin. Of course, it is of interest to find an estimate of the domain of stability when the origin is exponentially stable. Here, as an illustration, we compute an estimate of the domain of stability for $U = 19.0625$ m/s and

$a = -0.4$. For the choice of $Q = I_{6\times 6}$ in the Lyapunov Eq. (20), solving for $P > 0$ gives $\|PB\| = 141.1453$ and $\alpha^* = 0.055$ rad. Note that $\dot{V} < 0$ if the trajectory is such that $\alpha < \alpha^*$. When γ^* is computed from Eq. (30), it is found to be 0.018. Thus, the ellipsoid $E(\gamma)$, $\gamma < 0.018$, gives an estimate of the domain of stability, and if the perturbed initial state lies in $E(\gamma)$, then flutter is not possible. Using $\boldsymbol{x}(0) = [0, \alpha_0, 0, 0, 0, 0]^T$ in the level surface equation $E(\gamma^*) = \gamma^*$, one has $\alpha_0 = 1.0827$ deg. Thus, the initial condition $\boldsymbol{x}(0) = [0, 1.08 \text{ deg}, 0, 0, 0, 0]^T$ lies in the domain of attraction. Of course, the computed domain of stability is only an estimate.

Conclusions

In this Note, the question of existence of LCO of a prototypical aeroelastic wing section with structural nonlinearity in the pitch degree of freedom using the describing function approach has been considered. In the presence of asymmetric structural nonlinearity, the model exhibits asymmetric LCOs for certain values of flow velocities and locations of the elastic axis. When DIDF is used, limit cycles and associated oscillation parameters are obtained. For the flow velocities for which the origin is stable, stable and unstable limit cycles and an estimate of the domain of stability have been derived. It is seen that the unstable limit cycle has small amplitude and low frequency. Numerical results have been presented for a set of values of the flow velocities and the locations of the elastic axis that show that the predicated average value, amplitude, and frequency of LCOs are close to the actual values.

Appendix: System Parameters and Describing Function

System Parameters

The system parameters for simulation have been taken from Refs. 4 and 5:

$$b = 0.1064 \text{ m} \qquad m_w = 1.662 \text{ kg} \qquad c_h = 27.43 \text{ Ns/m}$$

$$c_\alpha = 0.036 \text{ Ns} \qquad \rho = 1.225 \text{ kg/m}^3 \qquad m_t = 12.387 \text{ kg}$$

$$I_\alpha = 0.04325 + m_w x_\alpha^2 b^2 \text{ kg} \cdot \text{m}^2 \qquad x_\alpha = [0.082 - (b + ab)]/b$$

$$s_p = 0.6 \text{ m}$$

$$k_\alpha = 2.82(1 - 7.8480\alpha + 663.2911\alpha^2 + 65.2754\alpha^3 - 4.9928 \times 10^3\alpha^4) \text{ N} \cdot \text{m/rad}$$

$$k_h = 2844.4 \text{ N/m}$$

Describing Function

The describing function has been obtained elsewhere[8] and is given by

$$(N_0/B_\alpha) = k_{\alpha_1}\left(0.5A_\alpha^2 + B_\alpha^2\right) + k_{\alpha_2}\left(1.5A_\alpha^2 B_\alpha + B_\alpha^3\right) + k_{\alpha_3}\left[3A_\alpha^2 B_\alpha^2 + B_\alpha^4 + 3A_\alpha^4(1/8)\right] + k_{\alpha_4}\left(5A_\alpha^2 B_\alpha^3 + B_\alpha^5 + (15/8)A_\alpha^4 B_\alpha\right)$$

$$N = 2k_{\alpha_1} B_\alpha + k_{\alpha_2}\left(0.75A_\alpha^2 + 3B_\alpha^2\right) + k_{\alpha_3}\left(3A_\alpha^2 B_\alpha + 4B_\alpha^3\right) + k_{\alpha_4}\left[7.5A_\alpha^2 B_\alpha^2 + 5B_\alpha^4 + (5/8)A_\alpha^4\right]$$

Acknowledgments

This research was supported by the U.S. Army Research Laboratory under Cooperative Agreement DAAAD19-03-2-007. The authors thank Thomas W. Strganac for providing the aeroelastic model parameters.

References

[1]Lee, B. H. K., Price, S. J., and Wong, Y. S., "Nonlinear Aeroelastic Analysis of Airfoils: Bifurcation and Chaos," *Progress in Aerospace Sciences*, Vol. 35, No. 3, 1999, pp. 205–334.

[2]Mukhopadhyay, V., "Historical Perspective on Analysis and Control of Aeroelastic Responses," *Journal of Guidance, Control, and Dynamics*, Vol. 26, No. 5, 2003, pp. 673–684.

[3]Lind, R., and Brenner, M., *Robust Aeroservoelastic Stability Analysis*, Springer-Verlag, London, 1999, Chap. 3.

[4]Ko, J., Kurdila, A. J., and Strganac, T. W., "Nonlinear Control of a Prototypical Wing Section with Torsional Nonlinearity," *Journal of Guidance, Control, and Dynamics*, Vol. 20, No. 6, 1997, pp. 289–301.

[5]Block, J., and Strganac, "Applied Active Control of a Prototypical Wing Section with Torsional Nonlinearity," *Journal of Guidance, Control, and Dynamics*, Vol. 20, No. 6, 1998, pp. 1181–1189.

[6]Marzocca, P., Librescu, L., and Silva, W. A., "Aeroelastic Response of Nonlinear Wing Sections Using a Functional Series Technique," *AIAA Journal*, Vol. 40, No. 5, 2002, pp. 813–823.

[7]Dowell, E., Edwards, J., and Strganac, T., "Nonlinear Aeroelasticity," *Journal of Aircraft*, Vol. 40, No. 5, 2003, pp. 857–874.

[8]Singh, S. N., and Brenner, M., "Limit Cycle Oscillation and Orbital Stability in Aeroelastic Systems with Torsional Nonlinearity," *Nonlinear Dynamics*, Vol. 31, No. 4, 2003, pp. 435–450.

[9]Theodorsen, T., "General Theory of Aerodynamic Instability and Mechanism of Flutter," NACA Rept. 496, 1935; also reprinted in *Aerodynamic Flutter*, edited by I. E. Garrick, AIAA Selected Reprint Series, Vol. 5, AIAA, New York, 1969, pp. 22–31.

[10]Gelb, A., and Van der Velde, W., *Multiple-Input Describing Functions and Nonlinear System Design*, McGraw–Hill, New York, 1968, Chap. 6.

[11]Slotine, J.-J., and Li, W., *Applied Nonlinear Control*, Prentice–Hall, Englewood Cliffs, NJ, 1991, pp. 80–81, 184–186.